Synthesis, Structure, and Magnetic Properties of the Low-Symmetry Tetranuclear Cubane-like Nickel Complex $[Ni_4(pypentO)(pym)(\mu_3\text{-}OH)_2(\mu\text{-}Oac)_2(NCS)_2(OH_2)]$

Juan M. Clemente-Juan, Benoît Chansou, Bruno Donnadieu, and Jean-Pierre Tuchagues*

Laboratoire de Chimie de Coordination, UPR CNRS 8241, 205 Route de Narbonne, 31077 Toulouse, France

Received May 23, 2000

The tetranuclear $[Ni_4(pypentO)(pym)(\mu_3\text{-}OH)_2(\mu\text{-}Oac)_2(NCS)_2(OH_2)]$ cubane-like complex has been prepared, and its structure and magnetic properties have been studied (pypentO and pym are the deprotonated forms of 1,5-bis[(2-pyridylmethyl)amino]pentane-3-ol and 2-pyridylmethanol, respectively). The X-ray diffraction analysis of this novel nickel complex ($C_{61}H_{74}N_{14}O_{25.5}S_4Ni_8$, monoclinic, $P2_1$, $a = 13.9375(14)$ Å, $b = 20.6604(18)$ Å, $c = 16.6684(19)$ Å, $\beta = 110.619(12)°$, $Z = 2$) showed a Ni_4O_4 cubane arrangement of four nickel atoms, four μ_3-O bridging ligands (one pypentO, one pym, and two OH^-), two syn−syn bridging acetates, and three terminal monodentate ligands (two NCS^- and one OH_2). In this low-symmetry elongated cubane, the four Ni−Ni long distances (3.18 Å) correspond to the faces of the cube including two μ_3-OR bridges, and the two Ni−Ni short distances (2.94 Å) correspond to the faces including two μ_3-OR and one acetate bridges. The temperature dependence of the magnetic susceptibility was fitted with $J_1 = -3.09$ cm^{-1}, $J_2 = 15.0$ cm^{-1}, $J_3 = 6.72$ cm^{-1}, and $g = 2.27$. The differences in sign among the J_1, J_2, and J_3 superexchange interactions is in good agreement with the different types of faces present in this Ni_4O_4 cubane core. The two faces of the cube, including two μ_3-OR bridges associated with one acetate bridge, exhibit ferromagnetic interactions, while the four faces which include only μ_3-OR bridges exhibit antiferromagnetic interactions. The very small zero field splitting may be attributed to the fact that the ground state is diamagnetic. The nature of the ground state is confirmed by the good simulation of the magnetization curves at 2 and 5 K (diagonalization of the full matrix taking into account all energy levels obtained with the parameter set resulting from the fit of the susceptibility curve). The large differences in J values resulting from small differences in Ni−O−Ni angles in this Ni_4O_4 core of very low symmetry reflect a quite strong magnetostructural correlation.

Introduction

Tetranuclear cubane-like nickel complexes have attracted considerable interest since the pioneering work of Andrew and Blake[1] and Ginsberg et al.[2] evidencing the presence of ferromagnetic interactions in a discrete tetranuclear compound. The cubane-like core of all studied tetranuclear nickel compounds includes four identical μ_3-O bridges arising either from OH[3] or OMe[1,2,4] or Oalkoxo[5] moieties. With the exception of three such compounds where additional multiatom bridging ligands slightly lower the symmetry,[3c,4c,e] the Ni_4O_4 core is highly symmetric, allowing one to consider that all intramolecular magnetic interactions are equivalent. The interaction is ferromagnetic (μ_3-OMe bridges, $\sim$7 cm^{-1})[1,2,4b] or antiferromagnetic (μ_3-OH bridges, -0.6 cm^{-1})[3b] for these highly symmetric compounds. On the other hand, the symmetry lowering requires consideration of two types of intramolecular magnetic interactions. In this case, the simultaneous occurrence of intramolecular ferro- and antiferromagnetic interactions has been ascribed to the differences in Ni−O−Ni angles: in agreement with the expectation that the Ni e_g electrons will couple ferromagnetically through oxygen p orbitals for Ni−O−Ni angles of 90°, the ferromagnetic interactions are associated with angles close to 90° (Ni−O−Ni = 95.85°, $J = 17.5$;[3c] Ni−O−Ni = 93.0°, $J = 17.5$;[4c] Ni−O−Ni = 96.7°, $J = 12.2$ [4e]), and the antiferromagnetic interactions are associated with larger angles (Ni−O−Ni = 103.2°, $J = -22$;[3c] Ni−O−Ni = 100.9°, $J = -9.1$;[4c] Ni−O−Ni = 99.6°, $J = -3.4$ [4e]). It is then remarkable to notice not only the large differences in J values resulting from small differences in Ni−O−Ni angles, but also the large range of J values in the case of the three cores of lower symmetry compared to those reported for Ni_4O_4 cores of higher symmetry. These observations prompted us to explore the possibility of further lowering the symmetry of the cubane Ni_4O_4 core by using a combination of pentadentate, bidentate, and monodentate ligands inspired from the results obtained during our study of the iron(II) chemistry with such mixed ligands.[6] In this contribution, we describe the preparation, characterization, X-ray crystal structure, and mag-

(1) (a) Andrew, J. E.; Blake, A. B. *J. Chem. Soc., Chem. Commun.* **1967**, 1174. (b) Andrew, J. E.; Blake, A. B. *J. Chem. Soc. A* **1969**, 1456.
(2) Bertrand, J. A.; Ginsberg, A. P.; Kaplan, R. I.; Kirkwood, C. E.; Martin, R. L.; Sherwood, R. C. *Inorg. Chem.* **1971**, *10*, 240.
(3) (a) Aurivillius, B. *Acta Chem. Scand. A* **1977**, 501. (b) Boyd, P. D. W.; Martin, R. L.; Schwarzenbach, G. *Aust. J. Chem.* **1988**, *41*, 1449. (c) Ballester, L.; Coronado, E.; Gutiérrez, A.; Monge, A.; Perpiñan, M. F.; Pinilla, E.; Rico, T. *Inorg. Chem.* **1992**, *32*, 2053.
(4) (a) Krüger, A. G.; Winter, G. *Aust. J. Chem.* **1970**, *23*, 1. (b) Barnes, J. A.; Hatfield, W. E. *Inorg. Chem.* **1971**, *10*, 2355. (c) Glandfelter, W. L.; Lynch, M. W.; Schaefer, W. P.; Hendrickson, D. N.; Gray, H. B. *Inorg. Chem.* **1981**, *20*, 2390. (d) Blake, A. J.; Brechin, E. K.; Codron, A.; Gould, R. O.; Grant, C. M.; Parsons, S.; Rawson, J. M.; Winpenny, R. E. P. *J. Chem. Soc., Chem. Commun.* **1995**, 1983. (e) Halcrow, M. A.; Sun, J. S.; Huffman, J. C.; Christou, G. *Inorg. Chem.* **1995**, *34*, 4167. (f) El Fallah, M. S.; Rentschler, E.; Caneschi, A.; Gatteschi, D. *Inorg. Chim. Acta* **1996**, *247*, 231.
(5) Bertrand, J. A.; Marabella, C.; Vanderveer, D. G. *Inorg. Chim. Acta* **1978**, *26*, 113. Paap, F.; Bouwman, E.; Driessen, W. L.; de Graaff, R. A. G.; Reedijk, J. *J. Chem. Soc., Dalton Trans.* **1985**, 737. Bizilj, K.; Hardin, S. G.; Hoskins, B. F.; Oliver, P. J.; Tiekink, E. R. T.; Winter, G. *Aust. J. Chem.* **1986**, *39*, 1035. Atkins, A. J.; Blake, A. J.; Schröder, M. *J. Chem. Soc., Chem. Commun.* **1993**, 1662.

10.1021/ic0005442 CCC: $19.00
Published on Web 11/03/2000

netic study of the tetranuclear $[Ni_4(pypentO)(pym)(\mu_3\text{-}OH)_2(\mu\text{-}Oac)_2(NCS)_2(OH_2)]$ cubane-like complex. The ligands pypentO and pym are the deprotonated forms of 1,5-bis[(2-pyridylmethyl)amino]pentane-3-ol and 2-pyridylmethanol, respectively.

Experimental Section

Materials. 3-Chloropropionyl chloride, sodium borohydride, 2-pyridinecarboxaldehyde (Aldrich), aluminum trichloride, nickel acetate tetrahydrate, potassium phthalimide, and potassium thiocyanate (Fluka) were used as purchased. High-grade solvents used for the synthesis of complexes were distilled prior to use.

Ligand. 1,5-Diaminopentane-3-ol dihydrochloride was synthesized according to a previously reported method.[7] The free 1,5-diaminopentane-3-ol was obtained by reacting the hydrochloride salt with the stoichiometric amount of freshly prepared sodium ethoxide in ethanol. The Schiff base condensation of 1,5-diaminopentane-3-ol (1 mmol) with 2-pyridinecarboxaldehyde (2 mmol) was carried out in ethanol (10 mL). The reaction mixture was stirred overnight, and the resulting Schiff base (orange solution) was reduced with 2 equiv of solid $NaBH_4$. The reaction mixture was warmed (60 °C) for 2 h and cooled to room temperature, and the salts were eliminated by filtration. The pypentOH ligand dissolved in the colorless filtrate was used without further purification.

Complex. A solution of $Ni(O_2CMe)\cdot 4H_2O$ (521 mg, 2.1 mmol) in EtOH (10 mL) was slowly added to a pypentOH ethanolic solution (2 mmol in 10 mL). The blue-green reaction mixture was stirred for a few minutes after which a solution of KSCN (220 mg, 2.1 mmol) in 1:1 MeOH/H_2O (5 mL) was added, and the mixture was stirred for an additional 15 min and filtrated. The resulting filtrate was allowed to stand for a few days during which blue single crystals of the title compound were obtained. Yield, 147 mg; 13.6%). Anal. Calcd (Found) for $C_{30}H_{50}N_7O_{13}S_2Ni_4$: C. 35.86 (36.75); H, 4.93 (4.23); N, 9.60 (9.48); S, 6.28 (5.78); Ni, 22.98 (22.66). Characteristic IR absorptions (KBr): 2087 ($\nu_{C=N}$), 1566, 1435 (ν_{COO}-), 877, 825 ($\nu_{C=S}$).

Crystallographic Data Collection and Structure Determination. The selected light-blue parallelepiped-shaped crystal was pasted on a glass fiber, mounted on a Stoe Imaging Plate Diffraction System (IPDS) using graphite-monochromated Mo Kα radiation, and equipped with an oxford cryostream cooler device. The data were collected at 160 K. Final unit cell parameters were obtained by least-squares refinement of a set of 5000 reflections ($I > 10\sigma(I)$), and the crystal decay was monitored by measuring 200 reflections per image. No significant fluctuations of diffracted intensities were observed during the measurement. A total of 29 361 reflections was collected, and 11 209 independent reflections ($R_{int} = 0.0380$) were used in the refinement.

The structure was solved by direct methods using SIR92 [8] and refined by least-squares procedures on F^2 with SHELXL-97[9] by minimizing the function: $\Sigma w(F_o^2 - F_c^2)^2$, where F_o and F_c are respectively the observed and calculated structure factors. The atomic scattering factors were taken from the International Tables for X-ray Crystallography.[10] All atoms were located on difference Fourier maps. All non-hydrogen atoms were refined anisotropically. The hydrogen atoms of the two amine functions of the pypentO$^-$ ligand, the hydrogen atoms of the two OH^-, and the two hydrogen atoms of the water molecule bonded to Ni3A and Ni3B have been refined with a fixed isotropic thermal parameter. All other hydrogen atoms were located on difference Fourier maps and placed in idealized positions with a fixed isotropic thermal parameter. A disorder has been found for the sulfur atom labeled S(1A), which could be refined on two positions with a 0.70/0.30 occupancy. An absolute configuration could not be assigned on the basis of the refinement of the Flack's parameter X[11] due to the value of this parameter which has been found close to 0.5; this result clearly indicates the presence of a twin by inversion center. This specific problem could be resolved by using the instruction TWIN with the matrix (−1 0 0, 0 −1 0, 0 0 −1) which expresses the twin law. Drawings of the molecule were performed with the program ZORTEP[12] with 30% of probability displacement ellipsoids for non-hydrogen atoms. Crystal data collection and refinement parameters are given in Table 1, and selected bond distances and angles are gathered in Table 2.

Table 1. Crystallographic Data for $[Ni_4(pypentO)(pym)(\mu_3\text{-}OH)_2(\mu\text{-}Oac)_2(NCS)_2(OH_2)]$

formula	$C_{61}H_{74}N_{14}O_{25.5}S_4\ Ni_8$
fw	2009.26
space group	$P2_1$ (No. 4)
a, Å	13.9375(14)
b, Å	20.6604(18)
c, Å	16.6684(19)
β, deg	110.619(12)
V, Å^3	4492.3(8)
Z	2
temp, K	160
λ, Å	0.710 73
r(calc), g cm^3	1.485
m, mm^{-1}	1.805
R_1[a]	0.0432
R_{w2} (F^2)[b]	0.1122

[a] $R_1 = \Sigma||F_o| - |F_c||/\Sigma|F_o|$. [b] $R_{w2} = \{\Sigma[w(F_o^2 - F_c^2)^2]/\Sigma[w(F_o^2)^2]\}^{1/2}$. $w = 1/[\sigma^2(F_o^2) + (0.0865P)^2 + 0P]$. $P = (F_o^2 + 2F_c^2)/3$.

Physical Measurements. Elemental analyses were carried out at the Laboratoire de Chimie de Coordination Microanalytical Laboratory in Toulouse, France, for C, H, N, and S and at the Service Central de Microanalyses du CNRS in Vernaison, France, for Ni. IR spectra were recorded recorded on a GX system 2000 Perkin-Elmer spectrophotometer. Samples were run as KBr pellets.

Magnetic data were obtained on powdered polycrystalline samples with a Quantum Design MPMS SQUID susceptometer. Magnetic susceptibility measurements were performed at 1T in the 2−300 K temperature range, and diamagnetic corrections were applied by using Pascal's constants. Isothermal magnetization measurements as a function of the external magnetic field were performed up to 5 T at 2 and 5 K. Least-squares fittings of the magnetic data were accomplished with an adapted version of the function-minimization program MINUIT.[13]

Results and Discussion

The molecular structure of the title compound is shown in Figure 1. The asymmetric unit includes two independent tetranuclear complex molecules, six H_2O, one methanol, and one ethanol molecules as crystallization solvent. Each complex molecule consists of an arrangement of four nickel atoms, four μ_3-O bridging ligands (one pypentO, one pym, and two OH^-), two syn−syn bridging acetates, and three terminal monodentate ligands (two NCS^- and one OH_2). The large number of ligands involved results in a cubane structure devoid of any point group element of symmetry. This low symmetry and the tetrahedric nature of the cubane core endows the tetranuclear complex molecule with chirality. In fact, the two independent complex molecules in the asymmetric unit are the two different isomers. These two isomers are alternatively packed into infinite chains due to the stacking of the pypentO and pym pyridines rings ~3.5 Å distant from each other.

(6) Clemente-Juan, J. M.; Mackiewicz, C.; Verelst, M.; Dahan, F.; Tuchagues, J.-P. Manuscript in preparation.
(7) Murase, I.; Hatano, M.; Tanaka, M.; Ueno, S.; Okawa H.; Kida, S. *Bull. Chem. Soc. Jpn.*, **1982**, *55*, 2404.
(8) Altomare, A.; Cascarano, G.; Giacovazzo, G.; Guagiardi, A.; Burla, M. C.; Polidori, G.; Camalli, M. Sir 92: Program for Automatic Solution of Crystal Structures by Direct Methods. *J. Appl. Crystallogr.* **1994**, 27, 435.
(9) Sheldrick, G. M. *SHELXL-97*: *Program for the Refinement of Crystal Structure;* University of Göttingen: Göttingen, Germany, 1997.
(10) *International Tables for X-ray Crystallography*; Kynoch Press: Birmingham, England, 1974; Vol. IV.
(11) Flack, H. D. *Acta Crystallogr.* **1983**, *A39*, 876.
(12) Zolnaï, L. *ZORTEP, Graphical Program for X-ray Structures Analysis*; University of Heidelberg: Heidelberg, Germany, 1998.
(13) James, F.; Roos, M. *MINUIT Program*, a System for Function Minimization and Analysis of the Parameters Errors and Correlations. *Comput. Phys. Commun.* **1975**, *10*, 345.

Table 2. Selected Bond Distances (Å), Angles (deg), and Torsion Angles (deg) for $[Ni_4(pypentO)(pym)(\mu_3\text{-}OH)_2(\mu\text{-}Oac)_2(NCS)_2(OH_2)]$

Ni(1A)−Ni(2A)	2.895(2)	Ni(1B)−Ni(2B)	2.901(2)
Ni(1A)−Ni(3A)	3.181(2)	Ni(1B)−Ni(3B)	3.188(2)
Ni(1A)−Ni(4A)	3.175(2)	Ni(1B)−Ni(4B)	3.186(2)
Ni(2A)−Ni(3A)	3.174(2)	Ni(2B)−Ni(3B)	3.185(2)
Ni(2A)−Ni(4A)	3.211(2)	Ni(2B)−Ni(4B)	3.183(2)
Ni(3A)−Ni(4A)	2.983(2)	Ni(3B)−Ni(4B)	2.977(2)
Ni(1A)−O(1A)	2.054(5)	Ni(1B)−O(1B)	2.048(5)
Ni(1A)−O(7A)	2.042(6)	Ni(1B)−O(4B)	2.087(5)
Ni(1A)−O(8A)	2.082(5)	Ni(1B)−O(7B)	2.056(5)
Ni(2A)−O(1A)	2.063(5)	Ni(2B)−O(1B)	2.060(5)
Ni(2A)−O(4A)	2.092(5)	Ni(2B)−O(7B)	2.069(5)
Ni(2A)−O(7A)	2.040(5)	Ni(2B)−O(8B)	2.064(5)
Ni(3A)−O(1A)	2.105(5)	Ni(3B)−O(1B)	2.124(4)
Ni(3A)−O(4A)	2.040(5)	Ni(3B)−O(4B)	2.048(5)
Ni(3A)−O(8A)	2.059(5)	Ni(3B)−O(8B)	2.050(5)
Ni(4A)−O(4A)	2.073(5)	Ni(4B)−O(4B)	2.066(5)
Ni(4A)−O(7A)	2.069(5)	Ni(4B)−O(7B)	2.058(5)
Ni(4A)−O(8A)	2.061(5)	Ni(4B)−O(8B)	2.072(5)
Ni(1A)−O(1A)−Ni(2A)	89.4(2)	Ni(1B)−O(1B)−Ni(2B)	89.8(2)
Ni(1A)−O(1A)−Ni(3A)	99.8(2)	Ni(1B)−O(1B)−Ni(3B)	99.6(2)
Ni(2A)−O(1A)−Ni(3A)	99.2(2)	Ni(2B)−O(1B)−Ni(3B)	99.2(2)
Ni(2A)−O(4A)−Ni(3A)	100.4(2)	Ni(1B)−O(4B)−Ni(3B)	100.9(2)
Ni(2A)−O(4A)−Ni(4A)	100.9(2)	Ni(1B)−O(4B)−Ni(4B)	100.2(2)
Ni(3A)−O(4A)−Ni(4A)	93.0(2)	Ni(3B)−O(4B)−Ni(4B)	92.7(2)
Ni(1A)−O(7A)−Ni(2A)	90.4(2)	Ni(1B)−O(7B)−Ni(2B)	89.4(2)
Ni(1A)−O(7A)−Ni(4A)	101.1(3)	Ni(1B)−O(7B)−Ni(4B)	101.5(2)
Ni(2A)−O(7A)−Ni(4A)	102.8(2)	Ni(2B)−O(7B)−Ni(4B)	100.9(2)
Ni(1A)−O(8A)−Ni(3A)	100.4(2)	Ni(2B)−O(8B)−Ni(3B)	101.5(2)
Ni(1A)−O(8A)−Ni(4A)	100.1(2)	Ni(2B)−O(8B)−Ni(4B)	100.6(2)
Ni(3A)−O(8A)−Ni(4A)	92.8(2)	Ni(3B)−O(8B)−Ni(4B)	92.5(2)
Ni(1A)−O(1A)−O(7A)−Ni(2A)	154.4(3)	Ni(1B)−O(1B)−O(7B)−Ni(2B)	154.8(3)
Ni(1A)−O(1A)−O(8A)−Ni(3A)	178.1(3)	Ni(1B)−O(1B)−O(4B)−Ni(3B)	177.1(3)
Ni(1A)−O(7A)−O(8A)−Ni(4A)	174.7(3)	Ni(1B)−O(4B)−O(7B)−Ni(4B)	176.5(3)
Ni(2A)−O(1A)−O(4A)−Ni(3A)	175.9(3)	Ni(2B)−O(1B)−O(8B)−Ni(3B)	176.8(3)
Ni(2A)−O(4A)−O(7A)−Ni(4A)	176.5(3)	Ni(2B)−O(7B)−O(8B)−Ni(4B)	175.9(3)
Ni(3A)−O(4A)−O(8A)−Ni(4A)	155.2(2)	Ni(3B)−O(4B)−O(8B)−Ni(4B)	154.3(2)

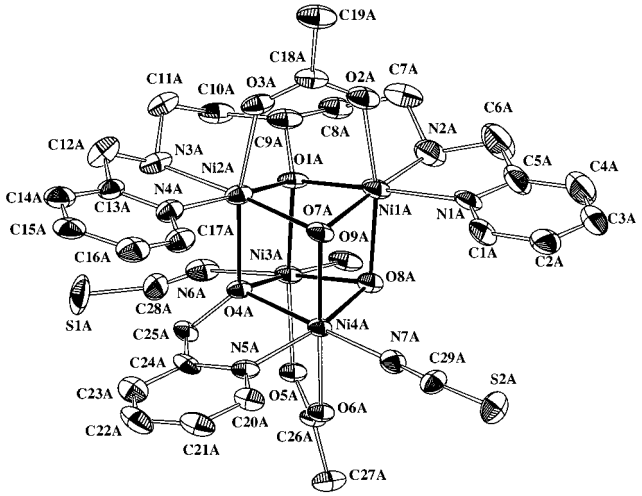

Figure 1. ORTEP view of the tetrameric unit A of $[Ni_4(pypentO)(pym)(\mu_3\text{-}OH)_2(\mu\text{-}Oac)_2(NCS)_2(OH_2)]$, with atom numbering scheme showing 30% probability ellipsoids.

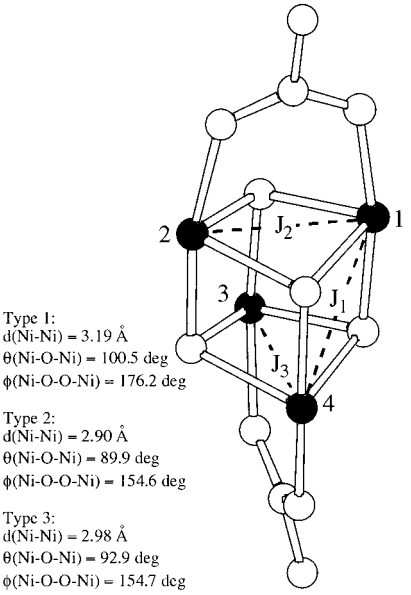

Figure 2. Schematic view of the $Ni_4O_4(Oac)_2$ core. Filled balls denote nickel atoms, and empty ones denote bridging oxygen atoms or acetate groups. Dashed lines show the three types of Ni···Ni exchange interactions (J_1, J_2, and J_3) based on the differences in structural parameters (Ni···Ni distances, Ni−O−Ni angles and Ni−O−O−Ni dihedral angles).

Taking into account only the Ni_4O_4 cubane core and the nature of the bridging ligands for the different faces of the cube, it is possible to assume a D_{2d} point group symmetry. In this elongated cube, the four Ni−Ni long distances (3.18 Å) correspond to the faces of the cube including two μ_3-OR bridges, and the two Ni−Ni short distances (2.94 Å) correspond to the faces including two μ_3-OR and one acetate bridges (Figure 2).

The magnetic properties have been investigated in the 2−300 K temperature range. The temperature dependence of both $\chi_M T$ and the molar susceptibility χ_M are represented in Figure 3. An antiferromagnetic behavior with a ∼14 K maximum in χ_M and a strong decrease at lower temperatures is observed. On the basis of a good magnetic isolation of the complex molecules from each other, the explanation of the diamagnetic nature of the ground state can be attributed to the antiferromagnetic interaction between the four $^3A_2$ nickel(II) ions. In a first step a symmetric

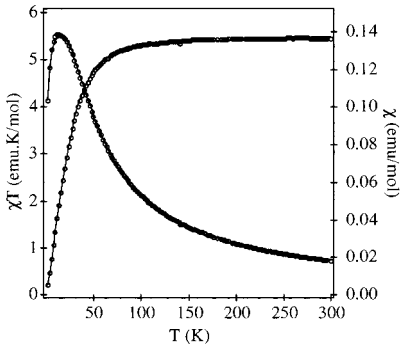

Figure 3. $\chi_M T$ product and χ_M vs T for $[Ni_4(pypentO)(pym)(\mu_3\text{-}OH)_2(\mu\text{-}Oac)_2(NCS)_2(OH_2)]$. Solid lines represent the best fit to the lower symmetry model (see text).

model (T_d) with only one averaged exchange parameter (J) and single-ion anisotropy parameter ZFS (D) was employed (eq 1). This model does not reproduce satisfactorily the susceptibility behavior.

$$\hat{H} = -2J\sum_{i=1}^{4}\sum_{j=i+1}^{4}\hat{S}_i\hat{S}_j + D\sum_{i=1}^{4}\hat{S}_i^2 \qquad (1)$$

A lower symmetry model (D_{2d}) is suggested by the differences in structural parameters among the faces of the cube (Figure 2). The corresponding network of exchange pathways is also shown in Figure 2, and eq 2 shows the Hamiltonian derived from this lower symmetry model.

$$\hat{H} = -2J_1(\hat{S}_1\hat{S}_3 + \hat{S}_1\hat{S}_4 + \hat{S}_2\hat{S}_3 + \hat{S}_2\hat{S}_4) - 2J_2\hat{S}_1\hat{S}_2 - 2J_3\hat{S}_3\hat{S}_4 + D\sum_{i=1}^{4}\hat{S}_i^2 \qquad (2)$$

Analytical expressions for eigenvalues and susceptibility cannot be derived due to the ZFS term. To calculate the energy levels and magnetic properties, diagonalization of the full matrix has been carried out.

A very good fit (not shown) can be obtained by using this lower symmetry model, the best set of parameters being $J_1 = -2.98$ cm^{-1}, $J_2 = 14.97$ cm^{-1}, $J_3 = 10.90$ cm^{-1}, $D = 0.011$ cm^{-1}, and $g = 2.23$. The low value of the ZFS parameter D may be attributed to the fact that the ground state is diamagnetic, and the ZFS is only involved in excited states. Consequently, the susceptibility experiment is hardly sensitive to this parameter, which contributes more to the susceptibility at high temperature when a large number of states are populated. For this reason we decided to fit the susceptibility data without taking into account axial single-ion anisotropy. The best fit was obtained for the following set of parameters: $J_1 = -3.09$ cm^{-1}, $J_2 = 15.0$ cm^{-1}, $J_3 = 6.72$ cm^{-1}, $g = 2.27$, a paramagnetic impurity of 4.1%, χ(TIP) per Ni(II) = 0.00024 cgs, and a residual (R) = 3.1×10^{-3} (solid lines in Figure 3).

The differences in sign among the J_1, J_2, and J_3 superexchange interactions is in good agreement with the three different types of faces present in this Ni_4O_4 cubane core (Figure 2). The two faces of the cube including two μ_3-OR bridges associated with one acetate bridge exhibit ferromagnetic interactions, while the four faces which include only μ_3-OR bridges exhibit antiferromagnetic interactions. The most important parameter considered in the magnetostructural correlation of the Ni_4O_4 cubane cores is the Ni−O−Ni angle. A ferromagnetic Ni−Ni interaction is observed when this angle is close to orthogonality.

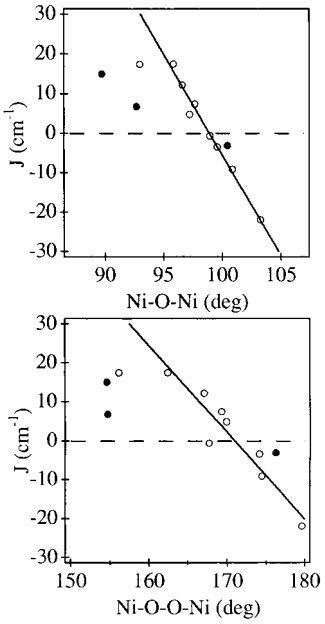

Figure 4. Exchange interaction for $[Ni_4(OR)_4]$ cubane cores as a function of Ni−O−Ni and Ni−O−O−Ni angles (open circles are literature data, and closed circles are from this work). Solid lines are the best fit obtained, and dashed lines are the border between ferro- and antiferromagnetic regions.

On the other hand, antiferromagnetic interactions have been observed for Ni−O−Ni bridging angles larger than 99°. As shown in Figure 2, the faces including both μ_3-OR and acetate bridges have a Ni−O−Ni angle close to orthogonality (89.9 and 92.9°), while the faces including exclusively μ_3-OR bridges have Ni−O−Ni angles close to 100°. The parameter set obtained from the fit fully confirms the soundness of this magnetostructural correlation.

The NiO−O−Ni dihedral angle has been suggested to be another structural parameter directly related to the sign of the exchange interaction, dihedral angles lower than 170° being associated with ferromagnetic interactions. The dihedral angles reported in Figure 2 clearly show that the fit parameters for the Ni_4O_4 cubane core reported in this study match the predicted signs derived from this second magnetostructural correlation.

Following the lead of Christou et al.,[4e] for comparison purpose, the magnetic interactions (J) are represented in Figure 4 as a function of averaged Ni−O−Ni angles for the different Ni_4O_4 cubane cores described in the literature and the one reported in this contribution. A linear dependence between J and the Ni−O−Ni angle is observed, and the antiferromagnetic parameter J_1 for the Ni_4O_4 cubane core reported in this contribution matches perfectly this linear dependence. The two other parameters (J_2 and J_3) do not match this linear dependence and show very low values with respect to the predicted one. This probably results from the effect of the acetate bridge which can mediate an additional exchange pathway and reduce significantly the ferromagnetic contribution. This effect has been reported previously for $[Ni_4(OCH_3)_4(OAc)_2(TMB)_4]^{2+}$ in which the presence of acetate bridges yields a 18 cm^{-1} ferromagnetic interaction for a Ni−O−Ni angle of 93°.[4c] For $[Ni_4(pypentO)(pym)(\mu_3\text{-}OH)_2(\mu\text{-}Oac)_2(NCS)_2(OH_2)]$, we observe two similar but distinct situations: the face including the μ_3-Opypent, μ_3-OH, and acetate bridges with Ni−O−Ni angles close to orthogonality (89.9°) and the face with two μ_3-OH and one acetate bridge with slightly larger Ni−O−Ni angles (92.9°). It is interesting to note that the J_2 (15.0 cm^{-1} for Ni−O−Ni ∼

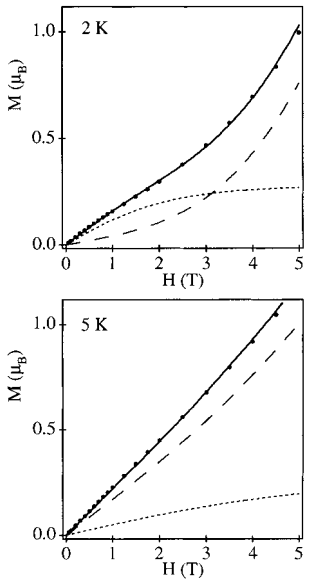

Figure 5. *M* vs *H* at 2 and 5 K for $[Ni_4(pypentO)(pym)(\mu_3\text{-}OH)_2(\mu\text{-}Oac)_2(NCS)_2(OH_2)]$. Solid lines represent the calculated curve from the best fit of χ_M vs *T* (lower symmetry model), dashed lines are the cubane contribution, and dotted lines are the paramagnetic impurity contribution.

89.9°) and J_3 (6.7 cm^{-1} for Ni−O−Ni ∼ 92.9°) values of the respective superexchange parameters clearly distinguish the two situations.

Finally, an additional proof of the nature of the ground state is the good simulation of the magnetization curves at 2 and 5 K (Figure 5). All energy levels obtained with the parameter set resulting from the fit of the susceptibility curve have been taken into account, and a diagonalization of the full matrix has been performed at each value of the magnetic field for the calculation of the theoretical curve[14] (the 4.1% ratio of $S = 1$ paramagnetic impurity has been taken into account with the corresponding Brillouin function).

From the minute study of this Ni_4O_4 core of very low symmetry, it may be concluded that the large differences in *J* values resulting from small differences in Ni−O−Ni angles really reflects a quite strong magnetostructural correlation. Also, the large range of *J* values in the case of the low-symmetry cores compared to those reported for Ni_4O_4 cores of higher symmetry is confirmed in this study. Due to the small number (2) of highly symmetrical Ni_4O_4 cores, the origin of the later observation remains an open question. However, in the case of highly symmetrical Ni_4O_4 cores, two characteristics deserve to be noted, (i) in both studied examples the Ni−O−Ni angle is quite large (97.7°,[1b,2] 99.0°[3a,b]), and (ii) while the μ_3-OR bridged core (97.7°) exhibits ferromagnetic interactions (7.5 cm^{-1}), the μ_3-OH bridged core (99.0°) exhibits antiferromagnetic interactions (−0.6 cm^{-1}).

Acknowledgment. The European Community is acknowledged for partial support through a postdoctoral grant to J.M.C.-J. within the framework of the TMR Contract FMRX- CT980174.

Supporting Information Available: Figures showing ORTEP views of the tetrameric units A and B of $[Ni_4(pypentO)(pym)(\mu_3\text{-}OH)_2(\mu\text{-}Oac)_2(NCS)_2(OH_2)]$, with atom numbering scheme and projections of the crystal structure in the *xy* and *yz* planes. The X-ray crystallographic file of $[Ni_4(pypentO)(pym)(\mu_3\text{-}OH)_2(\mu\text{-}Oac)_2(NCS)_2(OH_2)]$, in CIF format, is available. This material is available free of charge via the Internet at http://pubs.acs.org.

IC0005442

(14) Borrás-Almenar, J. J.; Clemente-Juan, J. M.; Coronado, E.; Tsukerblat, B. S. *Inorg. Chem.* **1999**, *38*, 6081.